Impacts of Autofluorescence on Fluorescence Based Techniques to Study Microglia

Haozhe Zhang
Zhengzhou University
Chen Tan
Zhengzhou University
Xiaoyue Shi
Zhengzhou University
Ji Xu (xuji@zzu.edu.cn)
Zhengzhou University https://orcid.org/0000-0002-6560-0491

Research Article

Keywords: microglia, autofluorescence, flow cytometry, immunofluorescence, live imaging

Posted Date: August 6th, 2021

DOI: https://doi.org/10.21203/rs.3.rs-731028/v1

Abstract

Microglia, the resident immune cells in the central nervous system, accrue autofluorescent granules inside their cytoplasm throughout their lifespan. In this report, we studied the impacts of autofluorescence on widely used fluorescence based techniques to study microglia, including flow cytometry, immunofluorescence staining and live imaging. The failed attempt of using fluorescein isothiocyanate (FITC) conjugated antibody to detect LAG3 protein in microglia prompted us to compare the sensitivity of FITC, PE and APC conjugated antibodies to detect surface protein expression in microglia. We found that phycoerythrin (PE) outperforms FITC and allophycocyanin (APC) as the fluorophore conjugated to antibody for flow cytometry by overcoming the interference from microglia autofluorescence. To identify the location and source of microglia autofluorescence, we did confocal imaging and spectral analysis of microglia autofluorescence on fixed brain tissues, revealing that microglia autofluorescence emits from cytoplasmic granules and displays a multi-peak emission spectrum. On live brain slices, autofluorescence could reduce the detected calcium signals imaged by GCaMP6s in microglia. In conclusion, autofluorescence is a critical factor to consider when designing experiments and interpreting results relying on fluorescence based techniques to study microglia.

Introduction

Microglia are tissue resident immune cells in the central nervous system. In physiological states, the branches and fine filopodias extended from somata and continuously survey the environment [1]. Once activated by pathological stimuli, microglia adopt functional alteration to either contribute or mitigate disease progression. Activated microglia can secrete a spectrum of chemokines and cytokines, which could affect other cells' function and survival in the central nervous system (CNS) [2, 3]. Microglia are also phagocytes, who engulf and digest the structures of damaged or stressed cells in the CNS [4]. By engaging these processes, microglia are an essential component of the development, homeostasis and disease progression in the central nervous system.

Fluorescence based techniques, including flow cytometry, immunofluorescence and live imaging, have been extensively employed to study microglia. Since microglia can be isolated from CNS single cell suspension, flow cytometry has always been a critical method to study protein expression in microglia. Flow cytometry using CD11b and CD45 antibodies can identify two distinct populations, $CD11b^{+}CD45^{medium}$ cells which represent parenchyma microglia derived from yolk sac progenitor cells and $CD11b^{+}CD45^{high}$ cells, which represent border associated macrophages or infiltrated macrophages derived from bone marrow monocytes. Surface expression of other investigated molecules in these populations can be further analyzed by multicolor flow cytometry after staining with antibodies conjugated with variant fluorophores. Excitation and emission spectrum, as well as quantum yields are main characteristics to consider when choosing fluorophores. Immunofluorescence technique has been used to study protein expression in microglia on fixed brain slices, commonly by co-staining the molecule under investigation and a microglia specific marker, such as IBA-1, TMEM119 and P2RY12 [5, 6]. Live

imaging on brain slices and in vivo has been employed to study microglia morphology, surveillance, migration and calcium signaling [7–10].

Lipofuscin like autofluorescent granules have been reported to accumulate in microglia from aging rodents, although the exact materials emitting autofluorescence are still not clear [11–13]. Microglia with autofluorescence actually represents a subset, which maintains their constant ratio throughout the animals' lifespan and have their unique photophysical, histological and functional properties [14]. However, how the autofluorescence would affect the fluorescence based techniques to study microglia has not been reported.

In this report, we studied how autofluorescence would affect flow cytometry, immunofluorescence and live fluorescence imaging of microglia. We found that application of Phycoerythrin (PE) conjugated antibodies allowed flow cytometry to have higher sensitivity than Fluorescein isothiocyanate (FITC) and Allophycocyanin (APC) conjugated antibodies to detect protein expression in microglia cells, by overcoming the interference from microglia autofluorescence. Imaging of microglia on fixed and live tissues revealed that cytoplasmic granules in microglia emitted autofluorescence. These autofluorescent granules from adolescent mice can potentially confound the interpretation of immunofluorescence results and reduce the sensitivity to detect calcium signals in microglia somata.

Methods

Animals

All mouse experiments were approved by the Animal Care and Use Committee at the Zhengzhou University. C57BL/6 mice, *Cx3cr1*^{GFP} mice (JAX # 005582) and Ai96(RCL-GCaMP6s) (JAX # 028866) mice were obtained from Jackson labs, Ltd. *Cx3cr1*^{CreER} mice were kindly provided by Dr. Steffen Jung from Weizmann Institute of Science. *Cx3cr1*^{GFP} and *Cx3Cr1*^{CreER} mice were maintained as heterozygous mice. Ai96 (RCL-GCaMP6s) were maintained as homozygous. *Cx3Cr1*^{CreER}: RCL-GCaMP6s were obtained by crossing *Cx3Cr1*^{CreER} heterozygous mice with Ai96 (RCL-GCaMP6s) homozygous mice and screening *Cx3Cr1*^{CreER} heterozygous offsprings by PCR genotyping. Tamoxifen (75 mg/kg) were given intraperitoneally for 5 consecutive days at the age of two months to activate CreERT2 recombinase, which can excise the stop cassette in the genomic DNA of Cx3Cr1CreER: RCL-GCaMP6s mice and thus allow the transcription of downstream GCaMP6s. LPS from Escherichia coli O127:B8 (Sigma, L5024) was injected intraperitoneally (5 μg/g body weight). All the experiments didn't distinguish between males and females.

Primary microglia isolation

Primary mouse microglia were isolated as previously described with slight modification [15]. In brief, Mice were euthanized and transcardially perfused with ice-cold 0.0356% heparin sodium solution. The brain was removed and placed in an EP tube containing ice cold 1X PBS. The whole brain was cut into pieces

with an ophthalmic scissor, blown into homogenate with a 5 ml syringe, and filtered with 70-μm filter. Brain homogenate was applied to a percoll gradient, and after a 30 min spin at 500 g, cells were collected from the 30%–70% interphase, pelleted, and washed.

Flow cytometry

Several strategies were used to block the suspected binding of antibody to Fcγ, including CD16/CD32 antibody (clone 93, Biolegend), CD16.2 antibody (clone 9E9, Biolegend) and mouse IgG (Solarbio). For antibody labeling, cells in the 200 μL ice cold 1× PBS were stained with CD11b (clone M1/70, BD Biosciences), CD45 (clone30-F11, Biolegend) and LAG-3 (clone C9B7W, Biolegend) or TIM-3 antibodies (clone RMT3-23, Biolegend) for 30 min on ice. Flow cytometry analysis was performed on a BD FACScanto. Data were analysed using FlowJo software (TreeStar).

Confocal imaging on fixed brain slices

Male and female mice were anesthetized with pentobarbital (100 mg/kg, i.p.) and transcardially perfused with PBS followed by 4% paraformaldehyde (PFA) in PBS, pH 7.4. Brains were post-fixed overnight in 4% PFA buffer, followed by cryoprotection in 30% sucrose in PBS for at least 48 h. Mouse brains were then embedded in Neg-50 frozen section medium (Fisher Scientific), sectioned using a cryostat at 60 μm and mounted on coverslips for confocal imaging.

For immunostaining for fluorescence microscopy, sections were washed 3 times in 0.1 m PBS for 10 min each, before being incubated in a blocking solution containing 5% NGS in 0.1 m PBS with 0.5% Triton X-100 for 1 h at room temperature on a shaker. For pretreatment of slices by lipofuscin quencher, slices were dipped in 1X TrueBlack® in 70% ethanol for 30 seconds. Sections were then incubated in Iba-1 antibodies (1:500; Wako) diluted in 0.1 M PBS with 0.5% Triton X-100 overnight at 4°C. The next day, the sections were washed 3 times in 0.1 m PBS for 10 min each before incubation at room temperature for 2 h with anti-rabbit 594 (1:500; Invitrogen) antibodies diluted in 5% NGS in 0.1 M PBS. The sections were then rinsed 3 times in 0.1 m PBS for 10 min each before being mounted on microscope slides.

Confocal fluorescence images were taken using Plan Apo 60× 1.4 NA oil-immersion objective lens and the Nikon A1 confocal laser-scanning microscope. We used the 488 nm laser to excite GFP, with the intensity adjusted to 1% of the maximum output. The emitted light pathway consisted of an emission band pass filter (500–550 nm) before the photomultiplier tube. Autofluorescence was excited by the 561 nm laser line at 1% of the maximum output. The emitted light pathway consisted of a 570–620 nm emission filter. The spectral images were taken by a A1-DUVB-2 GaAsP detector unit (400-720 nm, 10 nm per step).

2-photon imaging on live brain slices

For brain slice preparation, mice were deeply anesthetized with isoflurane and decapitated. Coronal brain slices (300 μm thickness) were prepared in chilled cutting solution comprising the following (in mM): 110

NaCl, 2.5 KCl, 1.25 NaH_2PO_4, 2 $CaCl_2$, 7 $MgCl_2$, 25 d-glucose, 75 sucrose bubbled with 95% O_2/5% CO_2. During incubation, the slices were submerged at room temperature in aCSF comprising the following (in mm): 126 NaCl, 25 $NaHCO_3$, 10 d-glucose, 2.5 KCl, 1.3 $MgCl_2$, 2.4 $CaCl_2$, and 1.24 NaH_2PO_4, bubbled with 95% O_2/5% CO_2. Brain slices were incubated in room temperature throughout the day. Slices were transfered to a recording chamber perfused with aCSF of a rate of 1–2 ml/min at 33°C.

2-photon fluorescence images were taken using Nikon NIR Apo 40× 0.8NA water immersion objective lens and the Nikon A1 multi-photon microscope. We used lock phased Coherent Chaemeleon 2-photon laser at 920 nm to excite GCaMP6s, with the intensity adjusted to 10% of the maximum output. The emitted light pathway consisted of an emission band pass filter (505–525 nm) before the IR NDD. The spectral images were taken by a A1-DUVB-2 GaAsP detector unit (400-720 nm, 10 nm per step).

Results

FITC conjugated antibody fails to detect LAG-3 expression in microglia

We first studied how autofluorescence would affect flow cytometry by studying lymphocyte-activation gene 3 (LAG-3) expression in microglia cells. The available RNA-seq data and our RT-PCR results have strongly suggested expression of LAG-3 mRNA in them (supplementary Fig. 1A) [16]. Since flow cytometry has been extensively used to study LAG-3 expression and function in T cells, we prepared single cell suspension from adult mice cortex and used flow cytometry to detect LAG-3 protein expression in microglia. FITC conjugated LAG-3 antibody was used for our purpose. Microglia cells were gated as $CD11^+/CD45^{low}$ cells from the brains of PBS injected mice (Fig. 1A, 1B). Then, FITC signals from isotype control antibody and LAG-3 antibody treated microglia were compared. From naive mice, FITC conjugated LAG-3 antibody treated microglia presented a negligible LAG-3 specific signal comparing to isotype control antibody treated ones (Fig. 1C). Since LPS induced inflammation can increase expression of certain inflammation related genes, we also performed flow cytometry on immune cells from the brains of mice injected with LPS intraperitoneally. Infiltrated lymphocytes from these mice, gated as $CD11^-/CD45^+$ cells, presented LAG-3 specific signal. We also observed that FITC signal from isotype control antibody treated lymphocytes was lower than that from microglia (Fig. 1D, 1E). Therefore, FITC conjugated LAG-3 antibody failed to detect LAG-3 protein in microglia from adult mice.

PE conjugated antibodies outperforms APC and FITC conjugated antibodies in detecting surface molecules in microglia

We speculated that non-specific binding of antibody to microglia may cause the high fluorescence background and lower the sensitivity of flow cytometry to detect LAG-3 specific signals from microglia. Antibodies can bind Fcγ receptors, so we blocked the suspected binding of antibody to Fcγ receptors by preincubating microglia with CD16/CD32 antibody and/or mouse IgG [17]. However, none of these procedures would lower the fluorescence signals from isotype control antibody treated microglia, thus

binding of antibody to Fcγ receptors was not responsible for the fluorescence signals from FITC conjugated isotype control antibody treated microglia **(Fig. 2A)**. We then suspected that the autofluorescence may be responsible for the background signals. Indeed, there was no difference of fluorescence intensities between naive microglia and FTIC conjugated isotype control antibody treated ones **(Fig. 2B)**. Therefore, autofluorescence caused the high fluorescent background in microglia cells and possibly lead to the failure of FITC conjugated LAG-3 antibody to detect LAG-3 protein in microglia.

We then tested LAG-3 antibodies conjugated with other fluorophores than FITC. Our results showed that PE conjugated LAG-3 antibody significantly improved the sensitivity of LAG-3 detection in microglia **(Fig. 2C, 2D)**. The ratio of median fluorescence intensity (MFI) of microglia treated with LAG-3 antibodies to its IgG control antibody, an indicator of sensitivity, was highest when antibody were conjugated with PE, while FITC and APC conjugated antibodies do not show a significant difference **(Fig. 2E)**. Therefore, among commonly used fluorophore, PE conjugated antibody outperforms APC and FITC conjugated antibodies in detecting surface molecules in microglia, by overcoming the interference from microglia autofluorescence.

We extended our observation to the detection of T cell immunoglobulin-3 (TIM-3), another immune checkpoint receptor in microglia by flow cytometry. RNA-seq data and the study from Anderson et al. also suggest TIM-3 to be expressed in microglia [16, 18]. PE conjugated TIM-3 antibody presented TIM-3 specific signals and higher sensitivity than FITC and APC conjugated antibodies **(Fig. 3A, 3B)**. Therefore, regardless of detection target, PE conjugated antibody has higher sensitivity than FITC or APC conjugated antibody to detect protein expression in microglia.

Microglia autofluorescence on fixed brain slices and its spectral properties

We expanded our study to identify the source of autofluorescence in microglia from adolescent mice and studied its impacts on fluorescence imaging of microglia cells in fixed brain tissues. We imaged microglia in the stratum radiatum of hippocampus CA1 region from fixed 7–9 weeks old *Cx3cr1*^{GFP} mice **(Fig. 4A)**. We can observe autofluorescent granules inside the cytoplasm of GFP positive cell by imaging fluorescence signals excited by a 561 nm laser and emitted through 595 nm/50 nm band pass filter **(Fig. 4B)**. Out of 16 microglia we imaged from three 7–9 weeks old mice, all contain autofluorescent granules. In addition, the autofluorescence in microglia can be removed by TrueBlack® lipofuscin autofluorescence quencher commercially available from Biotium (Fig. 4C, 4D).

We then applied spectral imaging on fixed brain slices to characterize the emission spectrum of microglia autofluorescence. Autofluorescence images were taken through 400–720 nm continuous bandpass filter, excited by 488 nm laser or 561 nm laser. When excited by 488 nm laser, autofluorescence from immunostained Iba-1 positive cells displayed multiple peaks on emission spectrum (500–520 nm, 540–550 nm, 570–630 nm, 650–690 nm) **(Fig. 4E)**. When excited by 561 nm laser, autofluorescence from GFP expressing cells of *Cx3cr1*^{GFP} mice displayed an emission spectrum similar to that excited by 488 laser with peaks at 570–630 nm and 650–690 nm **(Fig. 4F)**.

Autofluorescence can decrease calcium signals imaged by GCaMP6s on live brain slices

On live brain tissues, we imaged calcium signals in microglia cells from *Cx3Cr1*$^{Cre/ER}$: GCaMP6s mice, which selectively express genetically encoded calcium indicator (GECI) GCaMP6s in microglia **(Fig. 5A)** [19, 20]. Application of 100 μM UDP can increase calcium signals in microglia, indicated by increase of GCaMP6s fluorescence signals from microglia in hippocampus CA1 region **(Fig. 5B)**. Autofluorescent granules, which do not change their fluorescence intensities during UDP application, can be readily observed in GCaMP6s expressing microglia **(Fig. 5B)**. The amplitudes (F/F_0) of calcium signals induced by UDP application were significantly lower if autofluorescent granules were included to quantify the GCaMP6s fluorescent signal in microglia somata **(Fig. 5C, 5D)**. Therefore, strong autofluorescence emits from intracellular granules in microglia and reduces the observed calcium signals imaged by GCaMP6s. We also took the opportunity to acquire the emission spectrum of autofluorescent puncta from GCaMP6s expressing microglia on live brain slices, revealing emission spectrum with patterns similar to those acquired on fixed slices **(Fig. 5E)**.

Discussion

In the report, we studied how autofluorescence would affect the fluorescence based techniques to study microglia. First, we studied how flow cytometry would be affected by microglia autofluorescence. We systematically compared the sensitivity of FITC, PE and APC conjugated antibodies to detect protein expression in microglia and found that PE conjugated antibody has the highest sensitivity to detect protein expression in microglia. Therefore, due to the strong autofluorescence from microglia, the fluorophore conjugated to antibody for flow cytometry needs to be carefully selected to study microglia. The optical properties of both microglia autofluorescence and antibody conjugated fluorophores could possibly account for the higher sensitivity of PE conjugated antibodies to detect medium or low abundant protein expression in microglia. PE has relatively higher quantum yield than FITC and APC and thus was more capable of overcoming interference from autofluorescence. Our spectral imaging on microglia autofluorescence reveal an emission spectrum with multiple peaks, consistent with the mixed composition of lipofuscin. According to the emission spectrum of autofluorescence excited by 488 nm laser, the emission peak of PE (~570 nm) overlaps with one of the troughs of microglia autofluorescence emission spectrum, offering another explanation whey PE outperforms other fluorophores (Fig 4F).

We also found that the isotype control antibody (rat IgG1, kappa), which we have tested, doesn't bind to microglia, thus eliminating the necessity to use blockers, such as CD16/CD32 antibody, to block the potential binding of antibodies to Fcγ receptors. CD16/CD32 antibody can block FcγRs I, IIb, and III and CD16.2 antibody can bind FcγRIV. However, in our case, Rat IgG1 may not bind to either type of these Fcγ receptors. But it needs to be mentioned that this may not apply to antibodies with isotypes other than rat IgG1, especially because Biburger et al. reported that antibodies of different isotypes can have various binding capacity to FcγRIV [17].

Lipofuscin like autofluorescent granules have been reported to be accumulated in microglia from aged animals [11, 14]. Here we reported that autofluorescent granules can be observed in both fixed and live brain slices from young mice. Our experiments strongly supported that the substance emitting autofluorescence is lipofuscin. First, microglia autofluorescence is localized in cytoplasmic granules, consistent with lipofuscin stored in lysosomes; second, microglia autofluorescence can be removed by lipofuscin autofluorescence quencher; third, the multi-peak emission spectra of microglia autofluorescence agrees with the fact that lipofuscin is a mixture of partially digested proteins and lipids whose exact composition is still unknown.

Autofluorescent granules in microglia from fixed brain slices of young mice, where immunofluorescent stainings are usually performed, warn us to be cautious when interpreting the intracellular staining in microglia. It could be a concern that the autofluorescent puncta may be misidentified as engulfed materials, had proper control experiments not been performed. A few molecules have been shown to be engulfed by microglial and colocalized with $CD68^{+}$ lysosome structure by immunofluorescence techniques, including PSD95, synaptophysin, C1q, etc [21-23]. Our study has shown that autofluorescence quencher, such as the one from Biotium we used in this study, can remove the microglia autofluorescence, and thus should help the identification of intracellular puncta staining in microglia. The alternative strategy is to use antibody conjugating fluorophores with emission peak overlapping with the troughs of autofluorescence emission spectrum. According to our acquired emission spectrum of microglia autofluorescence, fluorophores such as Alexa555 (peak at 568 nm) or Alexa 633 (peak at 650 nm) should be able to overwhelm autofluorescence, when combined with an appropriate emission filter.

Live imaging of calcium signals in microglia have been performed by either loading calcium dye into the cells or selectively expressing genetically encoded calcium indicator in them [7-9]. The reason why autofluorescent granules have not been observed or reported in these studies can be high level of basal fluorescence emitted from calcium indicators or other fluorophores in these studies. The concentration of organic dye loaded into microglia cells by electrophoresis can be high enough to mask the endogenous autofluorescent granules. We imaged calcium signals in microglia by selectively expressing GCaMP6s in microglia. Due to the low basal calcium level, autofluorescent granules can be readily observed in microglia before UDP application. Umpierre et al used the similar strategy to express GCaMP6s in microglia, but with another *Cx3Cr1*^{CreER} mouse line, which express YFP in microglia and therefore may mask the autofluorescent granules [9].

Our study showed that autofluorescent granules exist in microglia from young mice, and they have profound impacts on fluorescence based methods, including flow cytometry, immunofluorescence and live imaging. Microglia autofluorescence can affect the sensitivity of flow cytometry to detect protein expression. Among PE, FITC and APC, PE conjugated antibody has the best ability to overcome the interference from microglia autofluorescence. Autofluorescent granules also need us to design immunofluorescence experiments and interpret results with care. Our live imaging experiments confirmed

the existence of autofluorescent granules in microglia and suggested that they can decrease the sensitivity of Ca^{2+} signal detection in microglia.

Declarations

-Funding: This work was supported by the National Natural Science Foundation of China grant (81870956) and National Key Research and Development Program of China (2018YFA0107303).

-Conflict of interest: The authors declare no conflicts of interest.

-Ethics approval/declarations: All mouse experiments were approved by the Animal Care and Use Committee at the Zhengzhou University.

-Consent to participate: not applicable.

-Availability of data and material/ Data availability: All data generated or analysed during this study are included in this published article and its supplementary information files.

-Code availability (software application or custom code): not applicable.

-Authors' contributions:

Haozhe Zhang: Data curation, Methodology, Writing- Original draft preparation.

Chen Tan: Data curation.

Xiaoyue Shi: Data curation.

Ji Xu: Conceptualization, Data curation, Supervision, Writing- Original draft preparation, Writing- Reviewing and Editing.

References

1. Nimmerjahn, A., F. Kirchhoff, and F. Helmchen, *Resting microglial cells are highly dynamic surveillants of brain parenchyma in vivo.* Science, 2005. **308**(5726): p. 1314-8.

2. Liddelow, S.A., et al., *Neurotoxic reactive astrocytes are induced by activated microglia.* Nature, 2017. **541**(7638): p. 481-487.

3. Giulian, D., et al., *Interleukin 1 of the central nervous system is produced by ameboid microglia.* J Exp Med, 1986. **164**(2): p. 594-604.

4. Damisah, E.C., et al., *Astrocytes and microglia play orchestrated roles and respect phagocytic territories during neuronal corpse removal in vivo.* Sci Adv, 2020. **6**(26): p. eaba3239.

5. Bennett, M.L., et al., *New tools for studying microglia in the mouse and human CNS.* Proc Natl Acad Sci U S A, 2016. **113**(12): p. E1738-46.

6. Werneburg, S., et al., *Targeted Complement Inhibition at Synapses Prevents Microglial Synaptic Engulfment and Synapse Loss in Demyelinating Disease.* Immunity, 2020. **52**(1): p. 167-182 e7.

7. Pozner, A., et al., *Intracellular calcium dynamics in cortical microglia responding to focal laser injury in the PC::G5-tdT reporter mouse.* Front Mol Neurosci, 2015. **8**: p. 12.

8. Eichhoff, G., B. Brawek, and O. Garaschuk, *Microglial calcium signal acts as a rapid sensor of single neuron damage in vivo.* Biochim Biophys Acta, 2011. **1813**(5): p. 1014-24.

9. Umpierre, A.D., et al., *Microglial calcium signaling is attuned to neuronal activity in awake mice.* Elife, 2020. **9**.

10. Haynes, S.E., et al., *The P2Y12 receptor regulates microglial activation by extracellular nucleotides.* Nat Neurosci, 2006. **9**(12): p. 1512-9.

11. Sierra, A., et al., *Microglia derived from aging mice exhibit an altered inflammatory profile.* Glia, 2007. **55**(4): p. 412-24.

12. Nakanishi, H. and Z. Wu, *Microglia-aging: roles of microglial lysosome- and mitochondria-derived reactive oxygen species in brain aging.* Behav Brain Res, 2009. **201**(1): p. 1-7.

13. Safaiyan, S., et al., *Age-related myelin degradation burdens the clearance function of microglia during aging.* Nat Neurosci, 2016. **19**(8): p. 995-8.

14. Burns, J.C., et al., *Differential accumulation of storage bodies with aging defines discrete subsets of microglia in the healthy brain.* Elife, 2020. **9**.

15. Ponomarev, E.D., et al., *Development of a culture system that supports adult microglial cell proliferation and maintenance in the resting state.* J Immunol Methods, 2005. **300**(1-2): p. 32-46.

16. Zhang, Y., et al., *An RNA-sequencing transcriptome and splicing database of glia, neurons, and vascular cells of the cerebral cortex.* J Neurosci, 2014. **34**(36): p. 11929-47.

17. Biburger, M., I. Trenkwald, and F. Nimmerjahn, *Three blocks are not enough–Blocking of the murine IgG receptor FcgammaRIV is crucial for proper characterization of cells by FACS analysis.* Eur J Immunol, 2015. **45**(9): p. 2694-7.

18. Anderson, A.C., et al., *Promotion of tissue inflammation by the immune receptor Tim-3 expressed on innate immune cells.* Science, 2007. **318**(5853): p. 1141-3.

19. Goldmann, T., et al., *A new type of microglia gene targeting shows TAK1 to be pivotal in CNS autoimmune inflammation.* Nat Neurosci, 2013. **16**(11): p. 1618-26.

20. Madisen, L., et al., *Transgenic mice for intersectional targeting of neural sensors and effectors with high specificity and performance.* Neuron, 2015. **85**(5): p. 942-58.

21. Dejanovic, B., et al., *Changes in the Synaptic Proteome in Tauopathy and Rescue of Tau-Induced Synapse Loss by C1q Antibodies.* Neuron, 2018. **100**(6): p. 1322-1336 e7.

22. Litvinchuk, A., et al., *Complement C3aR Inactivation Attenuates Tau Pathology and Reverses an Immune Network Deregulated in Tauopathy Models and Alzheimer's Disease.* Neuron, 2018. **100**(6): p. 1337-1353 e5.

23. Wang, C., et al., *Microglia mediate forgetting via complement-dependent synaptic elimination.* Science, 2020. **367**(6478): p. 688-694.

Figures

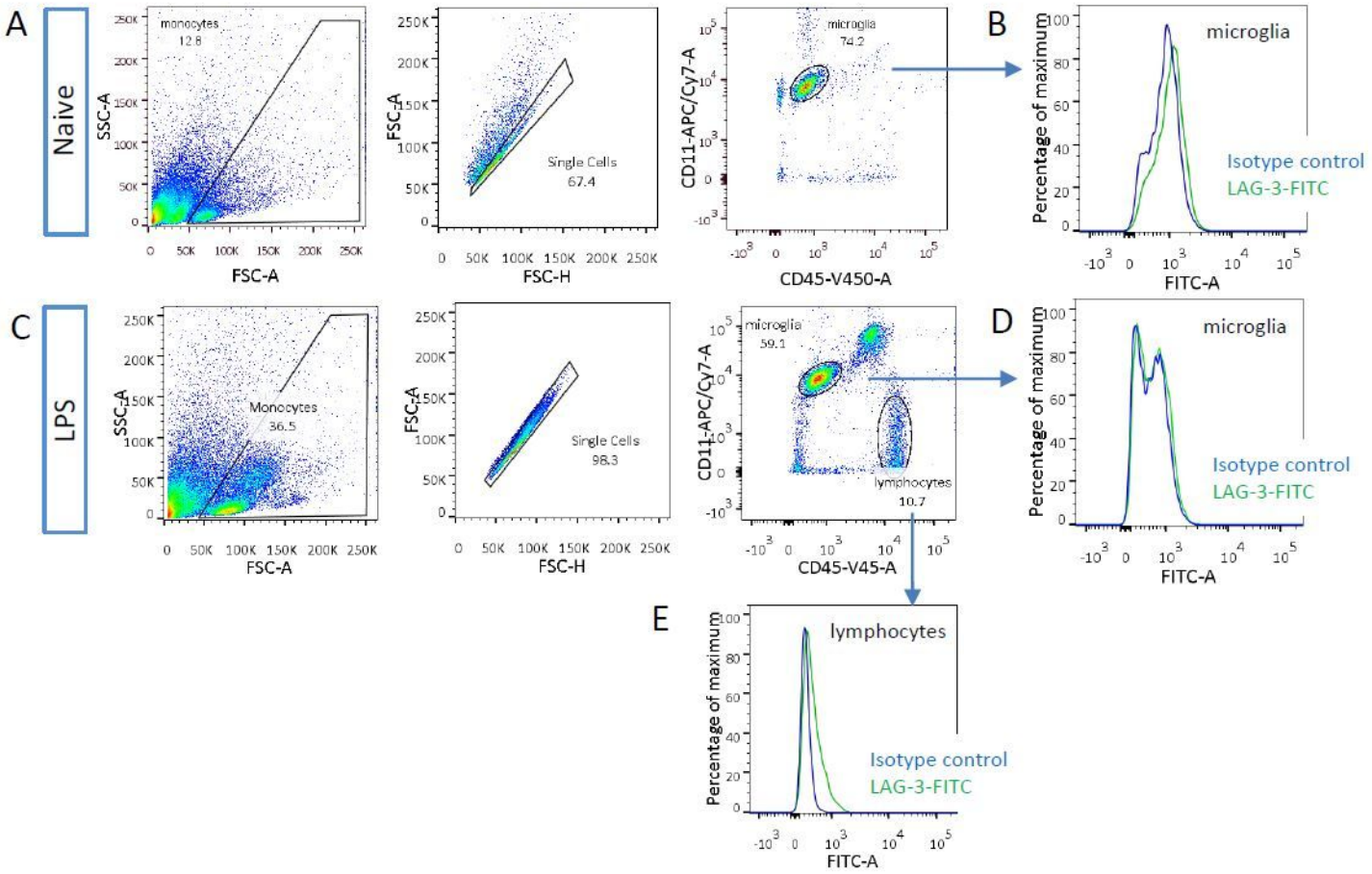

Figure 1

Gating strategies and detection of LAG-3 expression by FITC conjugated LAG-3 antibody. (A) Gating strategy of isolating single CD11+/CD45low cells from the brains of PBS injected mice. Single cell suspension from the brains of naïve mice involved pre-gating for side-scatter and single cells. Microglia were then identified by high expression of CD11b and low expression of CD45. (B) Distribution of

fluorescence intensities from FITC conjugated LAG-3 antibody and isotype control antibody treated microglia. (C) Gating strategy of isolating single CD11+/CD45low microglia cells and CD11-/CD45high lymphocytes from the brains of LPS injected mice. (D, E) Distribution of fluorescence intensities from FITC conjugated LAG-3 and isotype control antibody treated microglia (D) and lymphocytes (E) from LPS injected mice. All data were replicated in four independent experiments.

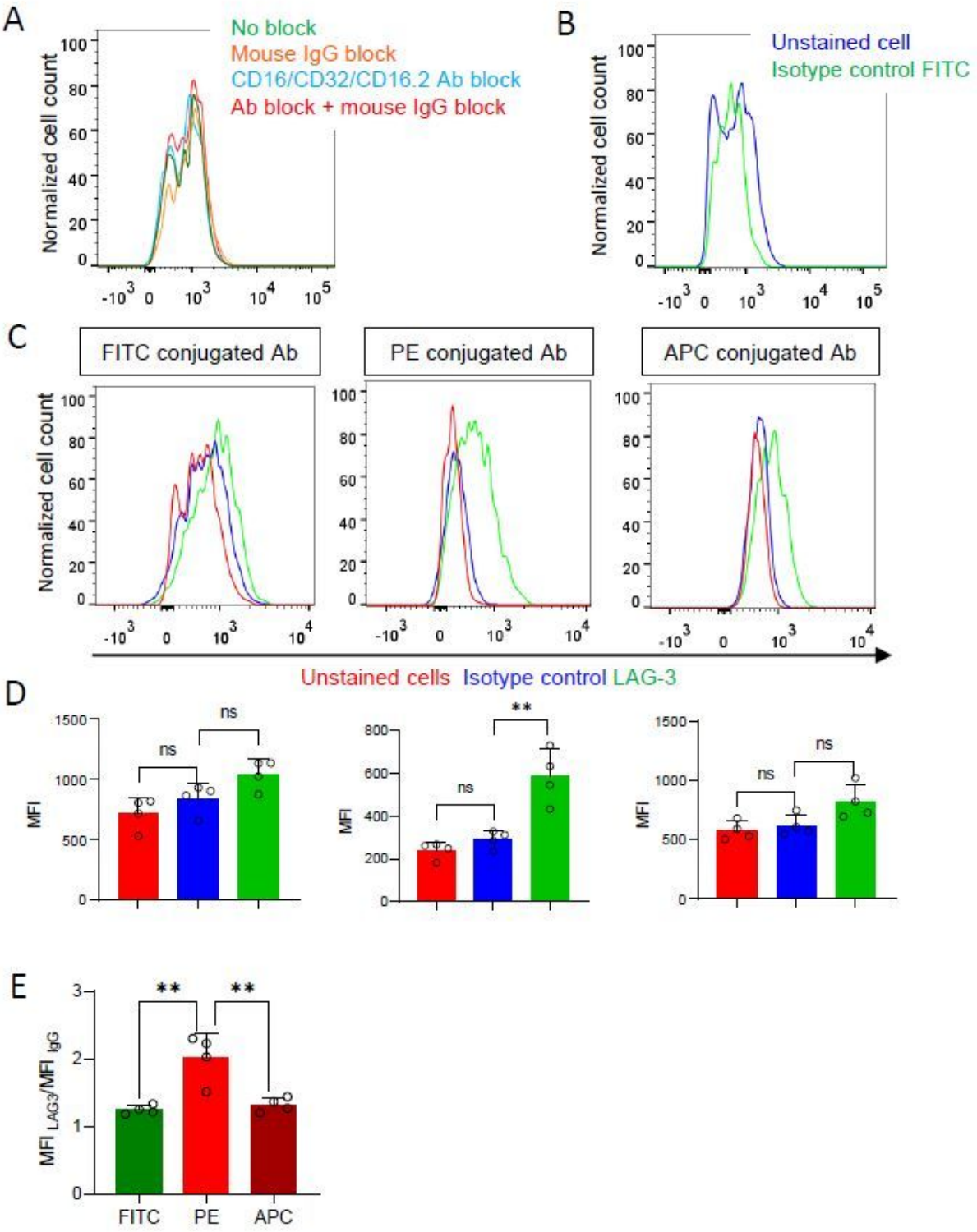

Figure 2

PE conjugated antibodies outperform FITC and APC conjugated antibodies in detecting microglia LAG3. (A) Distribution of fluorescence intensities from FITC conjugated isotype control antibody labeled microglia with previous blocking by mouse IgG, CD16/CD32/CD16.2 antibodies or the combination of mouse IgG and CD16/CD32/CD16.2 antibodies. (B) Distribution of fluorescence intensities from nontreated microglia and isotype control antibody treated microglia. (C) Distribution of fluorescence intensity from nontreated microglia and FITC, PE and APC conjugated LAG-3 antibodies and their respective isotype control antibodies treated microglia. (D) Median fluorescence intensity (MFI) of microglia as treated in (C). (E) Comparison of MFI LAG-3/MFI IgG of FITC, PE and APC conjugated LAG-3 antibodies. Bars represent means ± standard error of the mean (SEM). Comparisons were made by one-way ANOVA test with post hoc multiple comparisons. *P < 0.05, **P < 0.01. Data were collected from 4 mice.

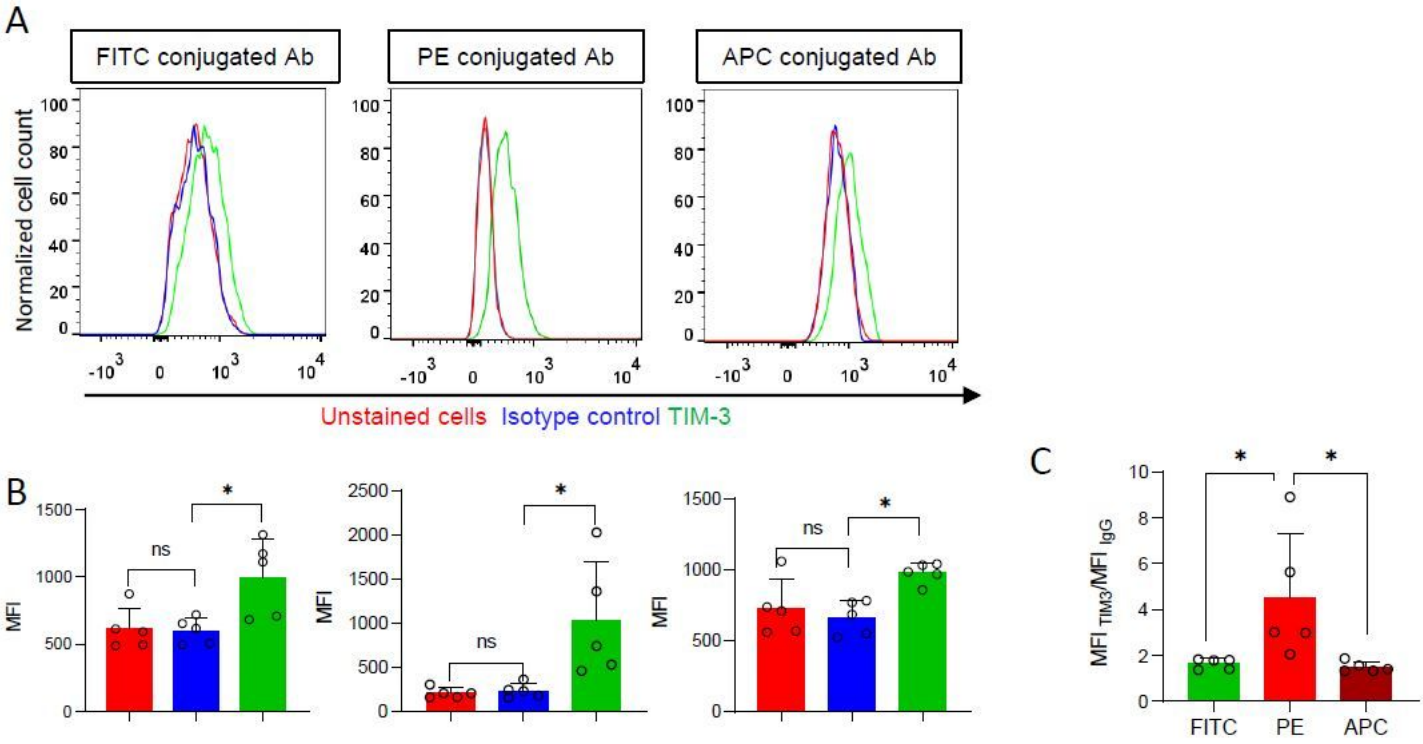

Figure 3

PE conjugated antibodies outperform FITC and APC conjugated antibodies in detecting microglia TIM-3. (A) Distribution of fluorescence intensities from nontreated microglia, FITC, PE and APC conjugated TIM-3 antibodies treated, and their respective isotype control antibody treated microglia. (B) The MFI of microglia treated as in (A). (C) Comparison of MFI TIM-3/MFI IgG of FITC, PE and APC conjugated TIM-3 antibodies. Bars represent means ± SEM. Comparisons were made by one-way ANOVA test with post hoc multiple comparisons. *P < 0.05, **P < 0.01. Data were collected from 5 mice.

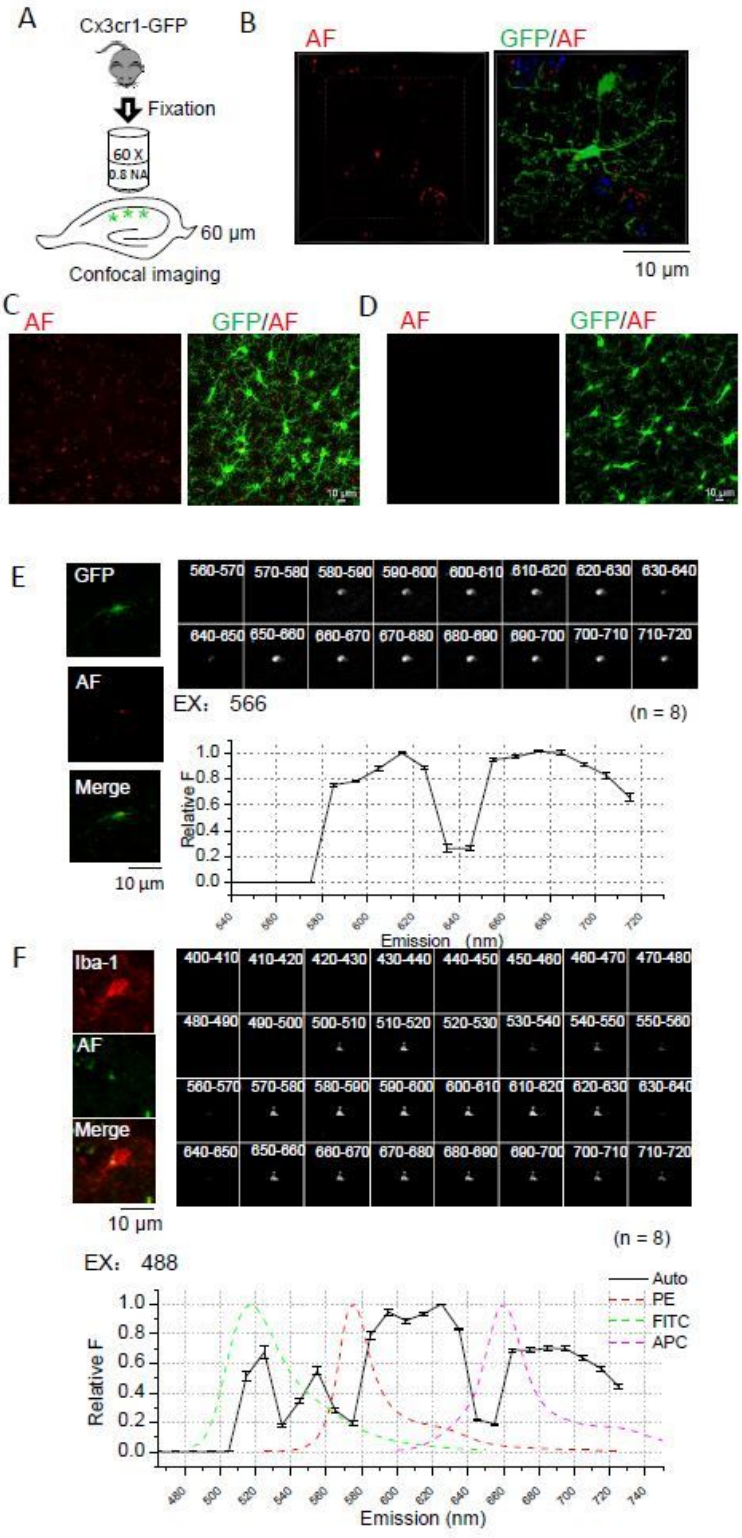

Figure 4

Spectral properties of microglia autofluorescent granules. (A) Diagram illustrates the imaging of hippocampus CA1 microglia on fixed brain slices. (B) 3D reconstruction of a microglia from 2 months old Cx3cr1GFP mouse with autofluorescence (AF) imaged in TRITC channel (561 nm laser, 595 nm/50 nm band pass filter). (C) Z projected image of stacks of microglia from Cx3cr1GFP mouse with auto fluorescence imaged as in panel (B). (D) Z projected stack images of microglia on slices with treatment

of true black before imaging. (E) Images of an autofluorescent granule from a GFP expressing microglia through continuous emission filter excited by 566 nm laser and its corresponding emission spectrum. (F) Images of an AF granule from a microglia labeled by Iba-1 antibody through continuous emission filter excited by 488 nm laser and its corresponding emission spectrum. Emission spectrum of FITC, PE and APC were shown for comparison. Bars represent means ± SEM. Data were collected from 3 mice.

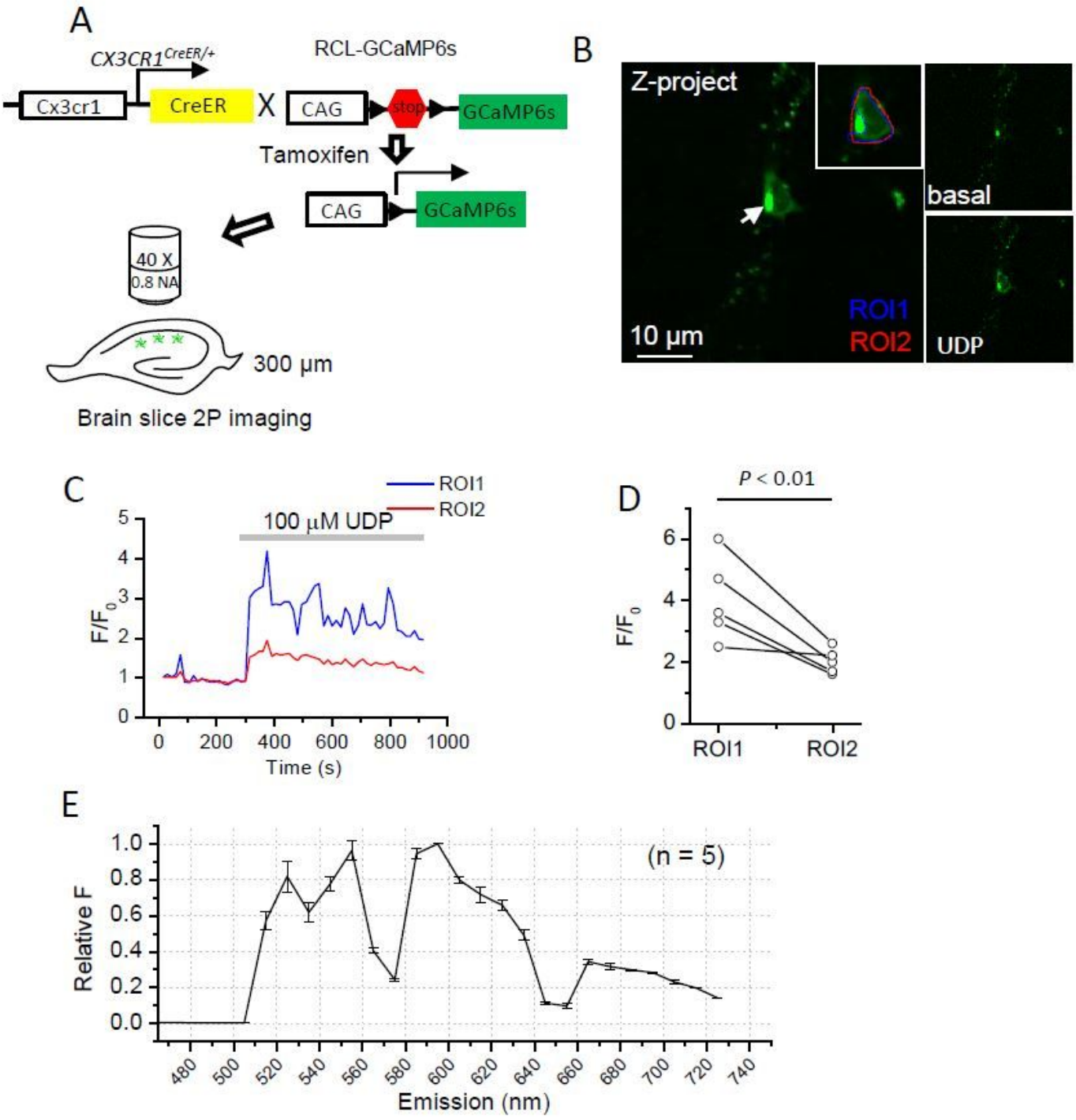

Figure 5

Microglia autofluorescence decreases calcium signal detected by GCaMP6s imaging in live brain slices (A) Diagram illustrates the strategy to image calcium signals in hippocampus CA1 microglia cells on live brain slices; (B) A represented Z-projected image of 60 GCaMP6s frames during 15 minutes imaging of a microglia on Cx3cr1CreER:GCaMP6s mouse brain slice. The arrow points to the soma of a microglia, which contains an autofluorescent granule. ROI1 circles the soma of microglia, excluding the autofluorescent granule, while ROI2 including it. Right top: the GCaMP6s image in basal condition. Right bottom: GCaMP6s image during application of 100 μM UDP. (C) F/F0 in ROI1 and ROI2 during 15 minutes imaging, at 5 minutes of which 100 μM UDP was applied. (D) The peak of F/F0 of GCaMP6s signals during UDP application in ROIs either excluding (ROI1) or including (ROI2) the autofluorescent granules. (E) Emission spectrum of the autofluorescent puncta as in panel (B) by spectral imaging. Bars represent means ± SEM. Data are collected from three mice and the comparison was made by paired t test.

Supplementary Files

This is a list of supplementary files associated with this preprint. Click to download.

- supp.figure1.jpg